



Title	GROWTH RATE OF CRYSTAL SURFACES WITH SEVERAL DISLOCATION CENTERS
Author(s)	Ohtsuka, Takeshi; Tsai, Yen-Hsi R.; GIGA, YOSHIKAZU
Citation	Hokkaido University Preprint Series in Mathematics, 1099, 1-25
Issue Date	2017-1-5
DOI	10.14943/84243
Doc URL	<a href="http://hdl.handle.net/2115/69903">http://hdl.handle.net/2115/69903</a>
Type	bulletin (article)
File Information	pre1099.pdf



[Instructions for use](#)

# GROWTH RATE OF CRYSTAL SURFACES WITH SEVERAL DISLOCATION CENTERS

TAKESHI OHTSUKA, YEN-HSI RICHARD TSAI, AND YOSHIKAZU GIGA

## 1. INTRODUCTION

We are interested in modeling and simulation of growth of crystal surfaces that have discontinuities in height along curves that spiral out from a few centers. The centers correspond physically to the end points of screw dislocation in the crystalline structure. Due to the dislocations, the crystal surface have discontinuities which are generally referred to as steps. Spiral steps evolve by catching atoms on the surface, and the increase in crystal height could be thought of as the spiral steps climbing up the helical surface provided by lattice structure of atoms including screw dislocations. We refer such type of crystal growth as “screw dislocation aided crystal growth”.

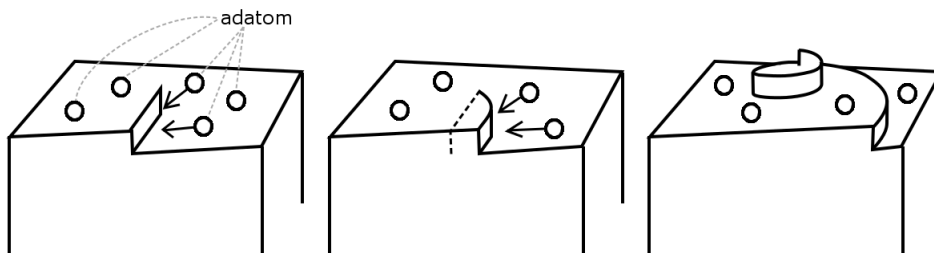


FIGURE 1.1. Illustration of crystal growth with aid of screw dislocation.

Since the spiral dynamics of several screw dislocations involve merging of different spirals, implicit interface methods are attractive options for description of the spiral steps. See [14, 15, 13] for details of the conventional level set methods, [3] for its foundation in mathematical analysis. For spiral curves, see the level set formulation introduced in [10] and [9]. On the other hand, a phase-field approach for evolving spirals are introduced by [5, 6, 7].

---

The first author is partly supported by the Japan Society for the Promotion of Science through grants No. 26400158(Kiban C).

The second author is partly supported by NSF grant DMS-1318975.

The third author is partly supported by the Japan Society for the Promotion of Science through grants No. 26220702(Kiban S) and No. 16H03948(Kiban B).

In this paper, we study the growth rates of such crystals as described in [1] using the method proposed in [9]. In particular, we give a quantitative definition of the critical distance (of co-rotating screw dislocations) under which the effective growth resembles that of a single spiral. We conclude that the critical distance in [1] is too small compared with our definition. We further give some improved estimates of the growth rate of crystal surface by co-rotating spirals. Finally, we present a numerical study on growth rates by a group of screw dislocations. In particular, the influence of distribution screw dislocations in a group of them is considered. Recently, Miura–Kobayashi [7] proposed a phase-field formulation for spiral crystal growth, and they concluded that their numerical simulations agree with the prediction of Burton et al [1]. One of the aims of this paper is to clarify some discrepancy between the growth rates computed by our method and those reported in [1] and [7]. Moreover, we study on the growth rate by a group including several rotational orientation, which is mentioned in [1] and not treated in [7].

The numerical simulations reported in this paper were computed by an implementation of the algorithm proposed in [9], and it is reviewed in the next section.

## 2. PRELIMINARIES

In this section we recall the level set method [10, 9] for evolving spiral steps by (2.1) on the crystal surface. The method also includes a way to reconstruct the crystal surface from the solution of the level set equation.

We consider a growing crystal surface that contains spiral steps attached to many screw dislocations. These steps are modelled as curves in  $\mathbb{R}^2$  in this paper, and we will use “curves” or “steps” interchangeably in this paper. According to the theory of Burton et al, [1], spiral steps move with normal velocities given as

$$(2.1) \quad V = v_\infty(1 - \rho_c \kappa),$$

where  $\kappa$  is the curvature corresponding to the inverse direction of the evolution of steps,  $v_\infty$  and  $\rho_c$  are positive constants describing the velocity of straight line steps and the critical radius of the two dimensional kernel, respectively.

When a single spiral step with a height,  $h_0 > 0$ , steadily rotates with angular velocity  $\omega$ , then the surface grows with the vertical growth rate

$$R = \frac{\omega h_0}{2\pi}.$$

Burton et al. [1] calculated  $\omega$  by approximating the form of the spiral step with an Archimedean spiral, and then they obtained that  $\omega = v_\infty/(2\rho_c)$ .

Our focus is naturally on the growth rate of crystals that evolve under the presence of many steps. In [1], some heuristic observation on such settings

were discussed. However, it was pointed out that the estimate on the growth rate for such setups was not accurate.

**2.1. Description of spirals.** Let  $\Omega$  be a bounded region in  $\mathbb{R}^2$ , and  $a_1, a_2, \dots, a_N \in \Omega$  be the centers of the spirals. Define

$$W = \Omega \setminus \bigcup_{j=1}^N \bar{B}_r(a_j),$$

where  $B_r(a_j)$  is a disc with radius  $r$  centering at  $a_j$ . We assume that  $\bar{B}_r(a_j)$  do not intersect.

In our method, spirals are implicitly defined by two functions,  $u$  and  $\theta$  as follows:

$$(2.2) \quad \Gamma_t := \{x \in \bar{W} \mid u(t, x) - \theta(x) = 2\pi n, \text{ for some integer } n\}.$$

Correspondingly, we define the orientation of a spiral by  $\mathbf{n} = -\frac{\nabla(u-\theta)}{|\nabla(u-\theta)|}$ .

$\theta(x)$  is a pre-determined function of the form

$$(2.3) \quad \theta(x) = \sum_{j=1}^N m_j \arg(x - a_j).$$

This function reflects the sheet structure of the lattice of atoms with screw dislocations, and it was first proposed by [6] to model spiral curves. The constants  $m_j$  define the strengths of the spiral centers: each strength is the difference between the strength,  $m_j^+$ , of counter-clockwise rotating spirals (that are attached to  $a_j$ ) and  $m_j^-$  for the clock-wise rotating ones. See [9, Definition 3,5] for details on  $m_j$ .

The function  $u(x, t)$  is called an auxiliary function to be approximated by solving a partial differential equation in  $W$  with suitable initial and boundary conditions:

$$(2.4) \quad u_t - v_\infty |\nabla(u - \theta)| \left\{ \rho_c \operatorname{div} \frac{\nabla(u - \theta)}{|\nabla(u - \theta)|} + 1 \right\} = 0 \quad \text{in } (0, T) \times W,$$

with an initial value condition  $u(0, x) = u_0(x)$  for  $x \in \bar{W}$  for a continuous function  $u_0$  on  $\bar{W}$  satisfying

$$(2.5) \quad \Gamma_0 = \{x \in \bar{W} \mid u_0(x) - \theta(x) = 2\pi n \text{ for an integer } n\}.$$

We impose the right angle condition between  $\Gamma_t$  and the boundary of  $W$ , which is denoted by  $\partial W$ . This condition is given as

$$(2.6) \quad \langle \vec{\nu}, \nabla(u - \theta) \rangle = 0 \quad \text{in } (0, T) \times \partial W,$$

where  $\vec{\nu}$  is the outer unit normal vector field of  $\partial W$ , and  $\langle \cdot, \cdot \rangle$  denotes the usual inner product in  $\mathbb{R}^2$ .

A few remarks are in order. First, the discontinuity of  $\theta$  does not cause any problem in (2.4) since  $\nabla\theta$  can be defined uniquely. In fact,  $\nabla\theta$  is well-defined on  $\overline{W}$  as

$$\nabla\theta = \sum_{j=1}^N \frac{m_j}{|x - a_j|^2} (-x_2 + a_{j,2}, x_1 - a_{j,1})$$

for  $x = (x_1, x_2)$  and  $a_j = (a_{j,1}, a_{j,2})$  by taking a branch of  $\theta$  so that it is smooth around  $x$ .

Second, notice that  $u_0$  satisfying (2.5) is not unique even if  $u_0$  is considered in the space of continuous functions. However, the uniqueness of  $\Gamma_t$  for a given  $\Gamma_0$  is established in [4] provided that  $u_0$  is continuous and the orientation of  $\Gamma_0$  given by  $u_0$  is same. In other words,  $\Gamma_t$  depends only on  $\Gamma_0$  and its orientation, and is independent of the choice of the functions that embed it.

**2.2. Growth rate of the surface.** With given  $\theta$  and  $u$ ,  $\Gamma_t$  is defined, and the height function the growing crystal surface is defined as

$$h = \frac{h_0}{2\pi} \theta_{\Gamma_t}(x),$$

where  $\theta_{\Gamma_t}$  is a branch of  $\theta$  that has  $2\pi$ -jump discontinuity only on  $\Gamma_t$ ; see [9]. We define the mean growth height in the time interval  $[t_0, t]$  as

$$H(t; t_0) = \frac{1}{|W|} \int_W (h(t, x) - h(t_0, x)) dx,$$

where  $|W|$  is the area of  $W$ . Here and hereafter we shall use a notation  $H(t) := H(t; 0)$  unless it is necessary to clarify the initial time  $t_0$ .

The growth rate of the crystal surface is then given formally by

$$R(t) = H'(t; t_0) = \frac{1}{|W|} \int_W h_t(t, x) dx.$$

However,  $H(t)$  may not be differentiable somewhere and may have oscillations with small amplitudes due to the domain shape. Therefore, in this paper, we computed an “effective” growth rate of the crystal by a linear approximation that best fit, in the sense of least square, the numerically computed values of  $H(t_j)$  for  $t_j$  in a chosen time interval. More precisely, we calculate  $R_\Delta$  minimizing

$$(2.7) \quad \min_{R_\Delta} \sum_{j=0}^K |H(t_0 + j\Delta t, t_0) - R_\Delta(j\Delta t - t_0)|^2$$

with  $\Delta t = (t_1 - t_0)/K$  for some  $K \in \mathbb{N}$  on a time interval  $[t_0, t_1]$ . Then, the coefficient  $R_\Delta$  gives the growth rate of the crystal surface in  $[t_0, t_1]$ .

### 3. NEW ESTIMATES OF THE GROWTH RATES AND NUMERICAL RESULTS

In this section, we discuss old and new estimates of crystal growth rates under different configurations of screw dislocations. Our discussion is accompanied by the corresponding numerical simulations which serve both as motivation and verification of the reported new results.

**3.1. Discretization and numerical parameters.** We discretize (2.4)–(2.6) on  $W \subset \Omega = [-1, 1]^2$  with a finite difference scheme using the Cartesian grids

$$D_s = \left\{ \left( \frac{i}{100s}, \frac{j}{100s} \right); -100s \leq i, j \leq 100s \right\} \subset \Omega = [-1, 1]^2$$

for  $s = 1, 2$ , or  $4$ . Denote the grid spacing by  $\Delta x = 1/100s$ . We solve the equation until  $T = 1$  using step size  $\Delta t := \Delta x^2/10$ . The spiral centers  $a_1, \dots, a_N$  are chosen from  $D_s$  and  $r < \Delta x$ . We calculate (2.4), (2.6) by the explicit finite difference scheme of the form

$$u_{i,j}^{k+1} = u_{i,j}^k + v_\infty (\mathbf{I}_{i,j}^k + \rho_c \mathbf{\Pi}_{i,j}^k),$$

where  $u_{i,j}^k = u(k\Delta t, i\Delta x, j\Delta x)$  and

$$\begin{aligned} \mathbf{I}_{i,j}^k &= \sqrt{|\tilde{\partial}_x(u - \theta)_{i,j}^k|^2 + |\tilde{\partial}_y(u - \theta)_{i,j}^k|^2}, \\ \mathbf{\Pi}_{i,j}^k &= \sqrt{|\hat{\partial}_x(u - \theta)_{i,j}^k|^2 + |\hat{\partial}_y(u - \theta)_{i,j}^k|^2} \left[ \operatorname{div} \frac{\nabla(u - \theta)}{|\bar{\nabla}(u - \theta)|} \right]_{i,j}^k. \end{aligned}$$

See [9, §3.1] for details of the difference formulae  $\tilde{\partial}_x w$ ,  $\hat{\partial}_x w$ , and  $\operatorname{div}(\nabla w / |\bar{\nabla} w|)$  for  $w = u - \theta$ . Note that in the formula of  $\tilde{\partial}_x w$  in [9, §3.1], the coefficient  $\delta (= \Delta x)$  in front of  $\mu$  is missing.

In this section we calculate the equation (2.4) with  $v_\infty = 6$  and various different values of  $\rho_c$  to obtain the evolution of spiral steps, i.e., spiral steps evolves by

$$V = 6(1 - \rho_c \kappa)$$

with some  $\rho_c$  for verifying our speculations. We also set  $h_0 = 1$ .

**3.2. Single spiral.** As the first test, we consider a situation where a single screw dislocation providing a single spiral step with the height of an atom. We call such a step *a unit spiral step*, and such a situation *a single spiral case*.

Burton et al. [1] pointed out that the growth rate of the crystal surface by a steadily rotating unit spiral step is

$$R^{(0)} = \frac{\omega h_0}{2\pi},$$

where  $\omega$  is the angular velocity of the rotating spiral. They estimated that  $\omega = \omega_1 v_\infty / \rho_c$ , and  $\omega_1 = 1/2$  with an approximation by an Archimedean spiral, or  $\omega_1 = \sqrt{3}/[2(1 + \sqrt{3})] \approx 0.315$  with an improved approximation. Cabrera and Levine [2] estimated that  $\omega_1 = 2\pi/19 \approx 0.330694$ , and this

number was referred to in [7]. Ohara and Reid [8] proposed to solve an ordinary differential equation in a half line to construct a spiral in  $\mathbb{R}^2$ . They use the shooting method to construct a solution and calculate  $\omega_1$  numerically as a shooting parameter. They obtained  $\omega_1 = 0.330958061$ . *In this paper, we assume that this quantity is more accurate physically and will use it as a reference in the following discussion.* We compare our computation to the angular velocity obtained by Ohara and Reid:

$$(3.1) \quad R^{(0)} = \frac{\omega_1 v_\infty h_0}{2\pi\rho_c}, \quad \omega_1 = 0.330958061.$$

In the simulations, we set  $N = 1$ ,  $m_1 = 1$ ,  $a_1 = 0$ , and

$$\theta(x) = \arg x.$$

In all of the evolutions presented in this paper, the height seems to grow linearly for  $t \geq 0.3$ . Figure 3.1 presents the computed height  $H(t) = H(t; 0)$  with  $\rho_c$  ranging from 0.03 to 0.1. We denote by  $R_\Delta$  the growth rate obtained from least square approximation of the computed height in the time interval  $[0.3, 1.0]$ . Table 1 shows some results comparing  $R_\Delta$  to  $R^{(0)}$ . We observe that the normalized differences  $e^{(0)} := |R_\Delta - R^{(0)}|/R^{(0)}$  decrease at a rate which is larger than first order in  $\Delta x$ .

Hereafter, we shall refer the above case ( $N = 1$ ,  $m_1 = 1$ ,  $a_1 = 0$ ) or results as a *unit spiral* case.

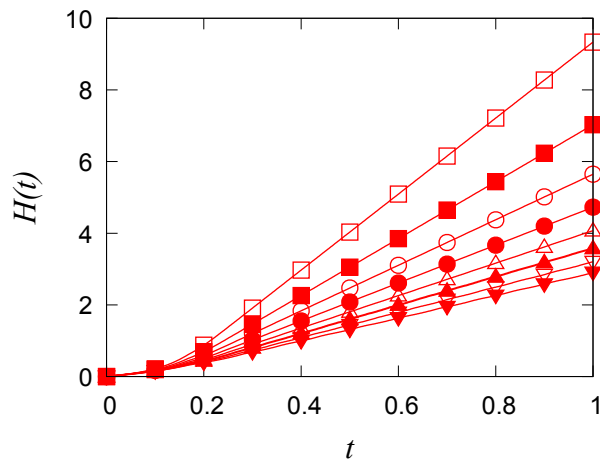


FIGURE 3.1. Graphs of  $H(t)$  for the evolution with a single screw dislocation and a unit spiral step. The horizontal axis means time  $t$ . Each line with a mark means the case  $\rho_c = 0.03(\square)$ ,  $0.04(\blacksquare)$ ,  $0.05(\circ)$ ,  $0.06(\bullet)$ ,  $0.07(\triangle)$ ,  $0.08(\blacktriangle)$ ,  $0.09(\nabla)$  and  $0.10(\blacktriangledown)$ , respectively.

TABLE 1. Normalized differences  $e^{(0)}$  from numerical growth rates to the theoretical values by a unit screw dislocation.

$\rho_c$	$e^{(0)}$		
	$s = 1$	$s = 2$	$s = 4$
0.030	0.006807	0.004024	0.001630
0.040	0.005830	0.002902	0.001064
0.050	0.005093	0.002164	0.000738
0.060	0.004021	0.001619	0.000542
0.070	0.003464	0.001281	0.000395
0.080	0.002875	0.001056	0.000349
0.090	0.002585	0.001044	0.000428
0.100	0.002128	0.000665	0.000144

**3.3. Co-rotating pair.** In the following, we study the dynamics of co-rotating pair of spirals and derive a new formula (3.7) for the growth rate for  $N$  co-rotating spirals. In Burton et al. [1], it is pointed out that the growth rate by a pair of co-rotating screw dislocations at  $a_1$  and  $a_2$  depends on the distance  $d := |a_1 - a_2|$  between the two screw dislocations. (Here we have interpreted “activity of screw dislocations” in [1] by “growth rate” on the above. Hereafter, we similarly continue to use this interpretation.) More precisely,

- (i) If the pair are far apart as  $d > 2\pi\rho_c =: d_c$ , then the growth rate by the pair is indistinguishable from that of a unit spiral, i.e.,  $R^{(0)}$ .
- (ii) If  $d \ll \rho_c$ , then the growth rate should be twice of  $R^{(0)}$ .

On one hand they do not mention on between of the above situations, on the other hand they estimated the growth rate of  $N$  co-rotating screw dislocations on a line with length  $L$  as

$$(3.2) \quad R^{(N)}(L) = \frac{N}{1 + L/(2\pi\rho_c)} R^{(0)}.$$

Our new formula gives a more accurate prediction of the critical distance separating the two cases mentioned above.

We first present a set of numerical simulations showing that the formula (3.2) is not accurate even for  $N = 2$ . Let

$$\theta(x) = \arg(x - a_1) + \arg(x - a_2)$$

for a given pair  $a_1 = (-\alpha, 0), a_2 = (\alpha, 0) \in \Omega$  with  $\alpha > 0$ . Set  $u_0 \equiv 0$ , so that the initial steps are on the opposite line segments of the line through  $a_1$  and  $a_2$ :

$$\Gamma_0 = \{a_1 + r(a_1 - a_2) \in \overline{W}; r > 0\} \cup \{a_2 + r(a_2 - a_1) \in \overline{W}; r > 0\}.$$



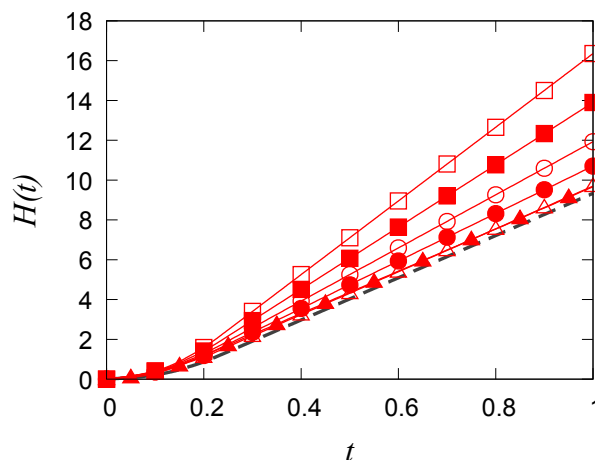


FIGURE 3.2. The left figure is the graphs of  $H(t)$  by a pair of co-rotating screw dislocations with  $\rho_c = 0.030$ . The line with  $\square$  means the case of  $d := |a_1 - a_2| = 0.04$ . Similarly, the line with  $\blacksquare$ ,  $\circ$ ,  $\bullet$ ,  $\triangle$ , and  $\blacktriangle$  means the case of  $d = 0.08$ ,  $0.14$ ,  $0.20$ ,  $0.30$  and  $1.00$ , respectively. Note that the graphs with  $d = 0.30$  and  $d = 1.00$  are agree with each other. The dashed line is  $H(t)$  of the unit spiral with the same  $\rho_c$ .

Figure 3.2 shows the graphs of  $H$  computed with  $\rho_c = 0.03$  in which we have  $2\pi\rho_c \approx 0.188496$ . From the Figure, we observe that the curves corresponding to  $d = 0.30$  and  $1.00$  are very close to that computed from a single spiral. Furthermore, they are quite far from the curve corresponding to  $d = 0.2$  (filled circles ( $\bullet$ ) in the figure). Since  $d = 0.2$  is larger than  $2\pi\rho_c$ , the numerical simulations suggest that the critical distance  $d_c$  is larger than  $2\pi\rho_c$ . In fact, the fitting lines for  $d = 0.20, 0.30, 1.00$  and the unit spiral for  $\rho_c = 0.03$  are

- $d = 0.20$ :  $H(t) \approx 11.926788t - 1.220501$ ,
- $d = 0.30$ :  $H(t) \approx 10.761760t - 1.061625$ ,
- $d = 1.00$ :  $H(t) \approx 10.611018t - 0.943661$ ,
- unit:  $H(t) \approx 10.606435t - 1.271220$ .

Miura and Kabayashi reported in [7] that they also found similar discrepancy using their phase field model. It is further pointed out, without providing an explicit formula, that the growth rate by a co-rotating pair is indistinguishable from that of the unit spiral if  $d \geq 3\pi\rho_c$ .

To clarify the cause of such discrepancy, we present here a heuristic derivation of (3.2) with  $N = 2$ , and with it we propose an improved formula for the growth rate, as well as the critical distance  $d_c$ . Note that, in the following we denote an angular velocity of a rotating spiral with (2.1) by  $\omega = \omega_1 v_\infty / \rho_c$ , where  $\omega_1$  is as in (3.1).

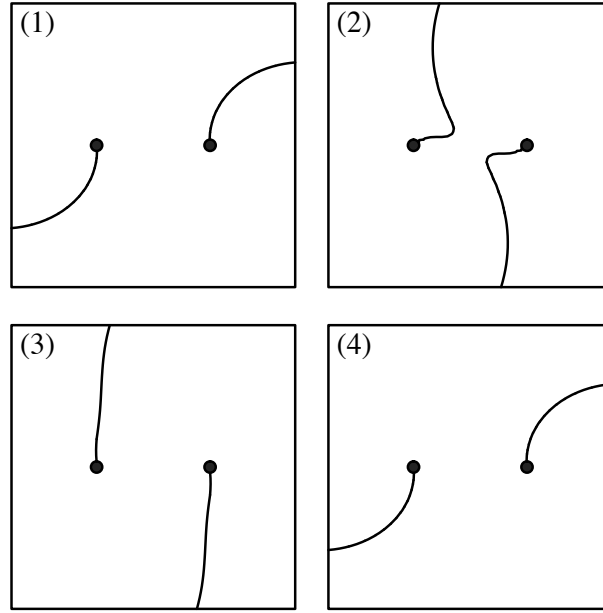


FIGURE 3.3. Process of rotation of co-rotating spirals.

- (i) The growth rate of a co-rotating pair with distance  $d = |a_1 - a_2|$  is given by

$$(3.3) \quad R^{(2)}(d) = \frac{2h_0}{T_d},$$

where  $T_d$  is the time that the pair of spiral steps goes rotating around the pair.

- (ii) There are two fundamental motion during the rotation of co-rotating spirals: switching spirals (from (1) to (3) in Figure 3.3) and half turn (from (3) to (4) in Figure 3.3). Twice of the switchings and the half turns occur during the rotation once, and then

$$T_d = 2(T_1 + T_2),$$

where  $T_1$  and  $T_2$  is the time for the switching and the half turn.

- (iii) We regard the switching motion as the end point of spirals moves from  $a_1$  to  $a_2$  with velocity  $v_\infty$ . Then,  $T_1 = d/v_\infty$ .  
 (iv) In the half turn, the angular velocity should be  $\omega = \omega_1 v_\infty / \rho_c$ . Then,  $T_2 = \pi / \omega = \pi \rho_c / (\omega_1 v_\infty)$ .  
 (v) Consequently we obtain

$$T_d = 2 \left( \frac{d}{v_\infty} + \frac{\pi \rho_c}{\omega_1 v_\infty} \right) = \frac{2d + 2\pi \rho_c / \omega_1}{v_\infty}.$$

By combining (3.3), (3.1) and the above we obtain

$$R^{(2)}(d) = \frac{2}{1 + d\omega_1/(\pi\rho_c)} \cdot \frac{v_\infty\omega_1 h_0}{2\pi\rho_c} = \frac{2}{1 + d\omega_1/(\pi\rho_c)} R^{(0)}.$$

Hence, for a pair of co-rotating spirals, we obtain the estimate of the growth rate

$$(3.4) \quad R^{(2)}(d) = \frac{2}{1 + d\omega_1/(\pi\rho_c)} R^{(0)}, \quad \omega_1 = 0.330958061,$$

where  $d$  is the distance between the two spiral centers which is assumed to be small. Furthermore, since  $R^{(2)}(d) < R^{(0)}$  if  $d > \pi\rho_c/\omega_1$ , the growth rate with a co-rotating pair should be revised as

$$(3.5) \quad \tilde{R}^{(2)}(d) = \begin{cases} R^{(2)}(d) & \text{if } d < \pi\rho_c/\omega_1, \\ R^{(0)} & \text{otherwise.} \end{cases}$$

Consequently, the critical distance is revised to

$$(3.6) \quad \tilde{d}_c = \frac{\pi\rho_c}{\omega_1}, \quad \omega_1 = 0.330958061.$$

We remark that with  $\omega_1 = 1/2$  the formulae (3.4) and (3.6) reduce to the predictions in [1].

For verification we report the normalized differences

$$e^{(0)}(d) := \frac{|R_\Delta(d) - R^{(0)}|}{R^{(0)}}, \quad e^{(2)}(d) := \frac{|R_\Delta(d) - R^{(2)}(d)|}{R^{(2)}(d)}$$

with respect to the distance  $d = |a_1 - a_2|$ . Again,  $R_\Delta$  computed by solving in (2.7) with the numerical data on  $t \in [0.3, 1.0]$ . The numerical simulations are performed with the centers

$$a_1 = (-k\Delta x, 0), \quad a_2 = (k\Delta x, 0) \quad (2 \leq k \leq 50),$$

where  $s = 1$ . Figure 3.4 presents numerical results of  $e^{(0)}(d)$  and  $e^{(2)}(d)$ . We observe that  $e^{(0)}(d)$  is small if  $e^{(2)}(d)$  is large, and inversely  $e^{(2)}(d)$  is small if  $e^{(0)}(d)$  is large.

From the numerical results we also can define the numerical critical distance  $\bar{d}_c$  dividing the co-rotating pair and independent two single spirals as

$$\bar{d}_c = \sup\{d; e^{(2)}(d) < e^{(0)}(d)\}.$$

From Figure 3.4 it seems that  $e^{(0)}(d)$  and  $e^{(2)}(d)$  crosses only once in all the cases, so that we now calculate  $\bar{d}_c$  with linear interpolation;

$$\bar{d}_c \approx \frac{Y_1 d_{\bar{k}} + Y_0 d_{\bar{k}+1}}{Y_1 + Y_0},$$

where  $\bar{k}$  is such that  $e^{(2)}(d_{\bar{k}}) \leq e^{(0)}(d_{\bar{k}})$  and  $e^{(2)}(d_{\bar{k}+1}) > e^{(0)}(d_{\bar{k}+1})$  for  $d_k = 2k\Delta x$ , and

$$Y_j = |e^{(0)}(d_{\bar{k}+j}) - e^{(2)}(d_{\bar{k}+j})|.$$

The computed results are tabulated in Table 2.

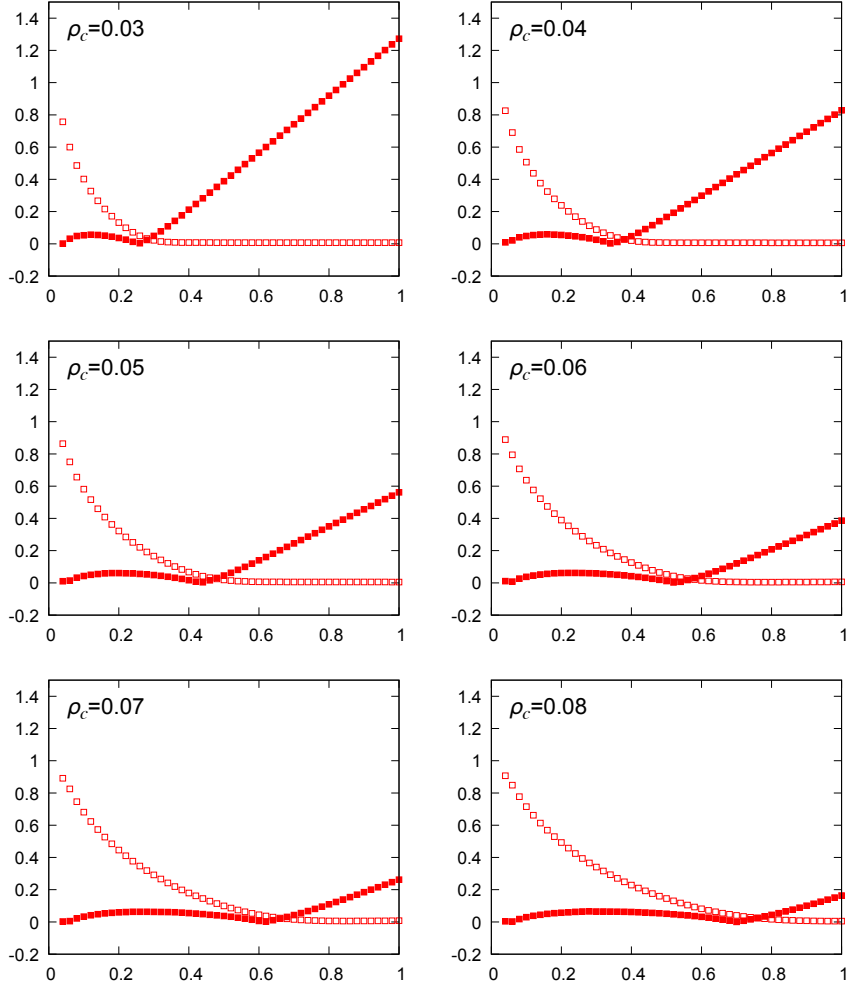


FIGURE 3.4. Graphs of normalized differences  $e^{(0)}(d)$  ( $\square$ ) and  $e^{(2)}(d)$  ( $\blacksquare$ ) for the pair  $a_1 = (-k\Delta x, 0)$ ,  $a_2 = (k\Delta x, 0)$  with respect to the distance  $d = |a_1 - a_2| = 2k\Delta x$ .

Note that the estimate (3.4) is still rough in the sense that

$$e_{dist} = \frac{|\bar{d}_c - \tilde{d}_c|}{\tilde{d}_c}$$

increase as  $\Delta x$  decreases; see Table 3. On the other hand, one finds that  $e^{(0)}$ , the normalized difference between the computed rate and the reference rate of a single spiral, approaches 1 as  $d \rightarrow 0$ . The limiting case corresponds to  $d = 0$  and  $\theta(x) = 2 \arg x$  is considered in [11], and it is proved that the growth rate of the surface is  $2R^{(0)}$  if the two spirals are unique up to a rotation.

TABLE 2. Comparison of the critical distances:  $d_c = 2\pi\rho_c$  used in [1], the revised distance  $\tilde{d}_c = \pi\rho_c/\omega_1$ , and the numerically observed critical distance  $\bar{d}_c$ .

$\rho_c$	$2\pi\rho_c$	$\tilde{d}_c$	$\bar{d}_c$
0.030	0.188496	0.284773	0.284813
0.040	0.251327	0.379697	0.379700
0.050	0.314159	0.474621	0.474650
0.060	0.376991	0.569545	0.569574
0.070	0.439823	0.664469	0.664486
0.080	0.502655	0.759394	0.759396

The numerical growth rates obtained in this subsection will be referred as  $R_{\Delta}^{(2)}$  in the following sections.

TABLE 3. Normalized differences of the critical distance between  $\tilde{d}_c$  and  $\bar{d}_c$ .

$\rho_c$	$e_{dist}$	
	$s = 1$	$s = 2$
0.030	0.000143	0.000275
0.040	0.000008	0.000013
0.050	0.000062	0.000108
0.060	0.000051	0.000094

**3.4. Pair with opposite rotations.** Consider the case that there is a pair of unit screw dislocations with opposite rotation. Burton et al. [1] pointed out on this case as follows.

- (i) If  $d = |a_1 - a_2| < 2\rho_c$  no growth occurs (called *inactive pair*).
- (ii) If  $d$  is around  $3\rho_c$ , then the growth rate is about  $1.1 \times R^0$ .
- (iii) If  $d \rightarrow \infty$ , then the growth rate decays exponentially to  $R^0$ .

We shall verify the above speculations numerically; in particular, on the estimate of the growth rate with the case (ii) of the above and on the distance attaining the maximal growth rate.

We first show the typical examples of the graphs of  $H(t)$  for pairs with opposite rotations in Figure 3.5. We present the numerical results using  $d = 0.10 < 2\rho_c$ , with  $\rho_c = 0.06$  on for case (i),  $d = 0.14 \in (2\rho_c, 3\rho_c)$  as the case between (i) and (ii),  $d = 0.18 = 3\rho_c$  and  $d = 0.24 = 4\rho_c$  as (ii), and  $d = 0.36, 1.0 \gg 3\rho_c$ . The dashed line in Figure 3.5 denotes the graph of  $H(t)$  on the unit spiral with  $\rho_c = 0.06$ . We find that the evolutions by the pair with opposite rotations is faster than the unit spiral, except the cases when  $d = 0.10$  and  $0.14$ .

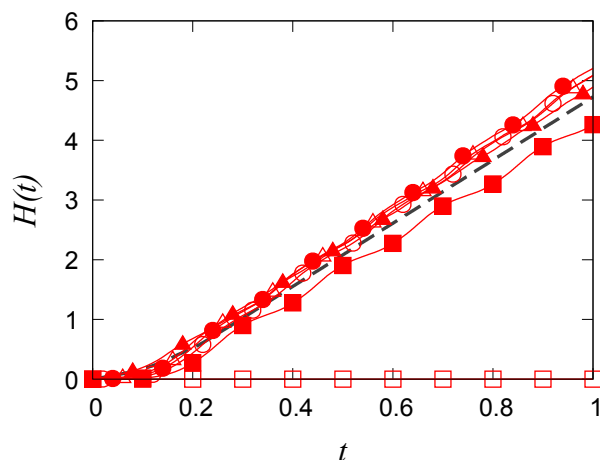


FIGURE 3.5. Graphs of  $H(t)$  for a pair with opposite rotations with  $\rho_c = 0.06$ . Each graph means that  $d = 0.10 < 2\rho_c(\square)$ ,  $d = 0.14 < 3\rho_c(\blacksquare)$ ,  $d = 0.18 = 3\rho_c(\circ)$ ,  $d = 0.24 = 4\rho_c(\bullet)$ ,  $d = 0.36(\triangle)$  and  $d = 1.0(\blacktriangle)$ . The dashed line denotes the graph of  $H(t)$  on the unit case spiral with  $\rho_c = 0.06$ .

To clarify the relation between  $d = |a_1 - a_2|$  and  $R_\Delta$ , we numerically estimate the rates  $R_\Delta$  for several  $\rho_c$  using computation performed in the time interval  $[0.3, 1.0]$ . In Fig 3.6 the red dots in each subplot correspond to  $R_\Delta$  computed with centers  $a_1 = (-k\Delta x, 0)$ ,  $a_2 = (k\Delta x, 0)$  for  $2 \leq k \leq 50$  and  $\Delta x = 0.01$ . Each subplot shows the computations using a different  $\rho_c$ . Thus, we observe that no growth occurs when  $d < 2\rho_c$  for the each case. By a similar argument as used in [12], one can prove that no growth would occur at the critical distance  $d = 2\rho_c$ . However, due to numerical errors, we observed slow growth at this critical distance from our computations. Our numerical simulations also show that, if  $d$  is around  $3\rho_c$ , the growth rate is larger than that corresponding to the unit spiral. In the subplots, the rate of the unit spiral is shown in the dashed lines.

In the column for  $s = 1$  in Table 4 we list the distance  $d^*$  at which the growth rate attains its maximum, and the normalized distance  $e^{(0)} = |R_\Delta - R^{(0)}|/R^{(0)}$  between  $R_\Delta$  and  $R^{(0)}$  at  $d = d^*$ . We find  $e^{(0)}$  is around 0.1, and the maximum growth rate around  $1.1 \times R^{(0)}$ , agreeing with [1] or [7]. However, we also find that the all results of  $d^*/\rho_c$  examined here are between 3.5 and 4, which are larger than that value described in [1] or [7]. See also Figure 3.7, which shows the relation between  $R_\Delta/R^{(0)}$  and  $d/\rho_c$  for  $\rho_c = 0.06$  and  $0.08$  with  $s = 2$ .

**3.5. Group on a line.** In this section we consider a situation where co-rotating screw dislocations  $a_1, \dots, a_N$  with a unit spiral step is ordered on

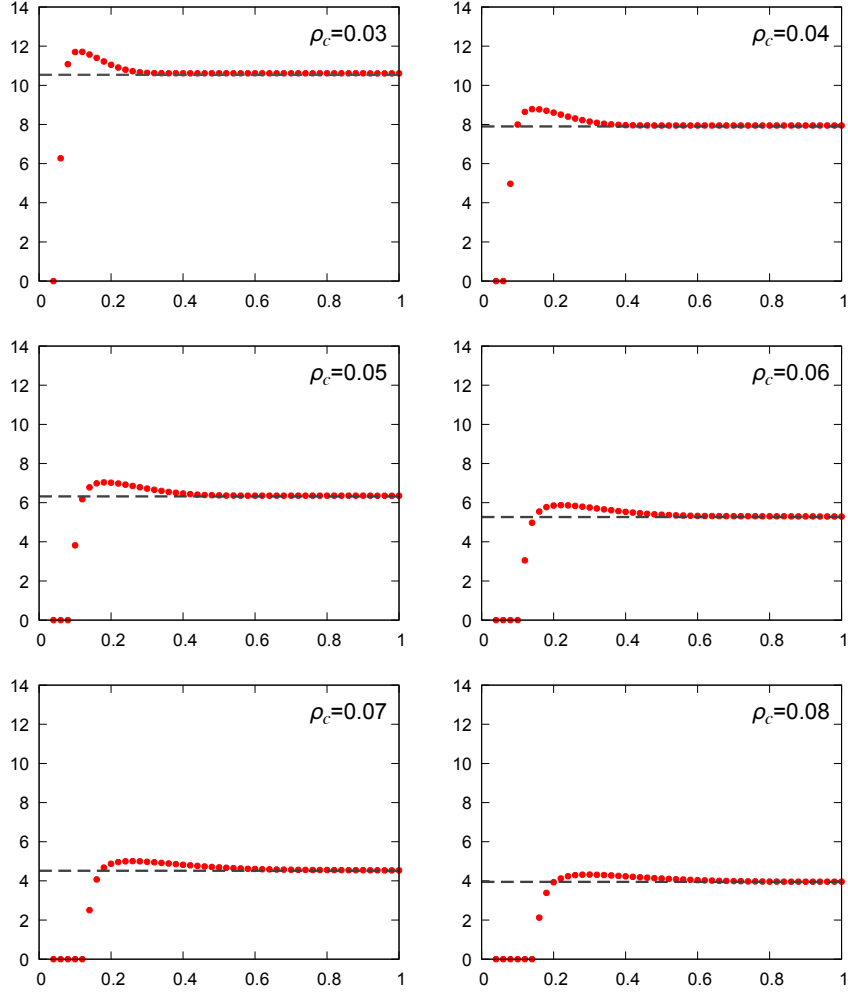


FIGURE 3.6. Graphs of  $R_\Delta$  as a function of  $d = |a_1 - a_2|$ . The dashed line means  $R^{(0)}$  for the each case.

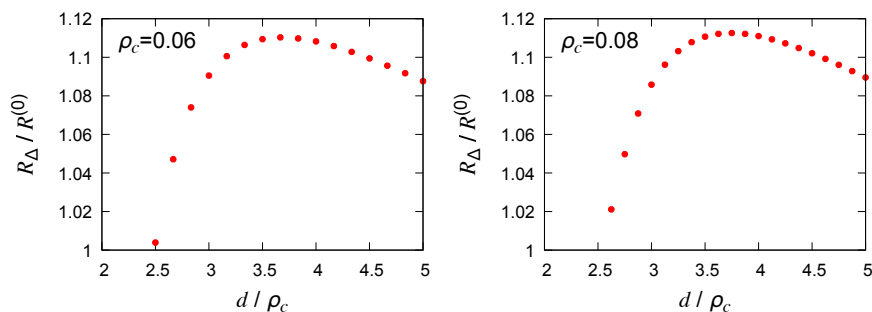
a line, i.e., there exists  $\lambda_j$  such that  $0 = \lambda_1 < \lambda_2 < \dots < \lambda_N = 1$  and  $a_j = (1 - \lambda_j)a_1 + \lambda_j a_N$ . Burton et al. [1] estimated the growth rate by such a  $a_1, \dots, a_N$  as (3.2) if  $|a_{j+1} - a_j| < d_c$  for each  $j = 1, \dots, N - 1$  and  $|a_1 - a_N| = L$ . Then, by similar argument to obtain (3.4) as in §3.3, we obtain the improved estimate of (3.2) as

$$(3.7) \quad R^{(N)}(d) = \frac{N}{1 + L\omega_1/(\pi\rho_c)} R^{(0)}, \quad \omega_1 = 0.330958061.$$

We here remark that the estimate (3.7) in [1] is independent of the distribution of  $a_j$ 's on the line. In [7], the authors investigated the consistency

TABLE 4. The distance between a pair of centers that result the maximal growth rate on a pair with opposite rotations.

$\rho_c$	$s = 1$		$s = 2$	
	$d^*$	$e^{(0)}$	$d^*$	$e^{(0)}$
0.030	0.120	0.111637	0.120	0.083197
0.040	0.140	0.111348	0.150	0.107062
0.050	0.180	0.113245	0.180	0.108329
0.060	0.220	0.114888	0.220	0.110311
0.070	0.260	0.108985	0.260	0.104386
0.080	0.300	0.094041	0.300	0.112575

FIGURE 3.7. Graphs showing relation between  $R_\Delta/R^{(0)}$  and  $d/\rho_c$  for  $\rho_c = 0.06$  and  $0.08$  with  $s = 2$ .

of the above formula and presented numerical simulations for several co-rotating screw dislocations ( $N \geq 2$ ) with  $\omega_1 = 2\pi/19$  and equally arranged dislocations. However, actually the distribution of screw dislocations has influence to the growth rate. We present below numerical results verifying this assertion.

Consider the situation  $N = 3$  and  $\tilde{d}_c < |a_1 - a_3| < 2\tilde{d}_c$ , for example,

$$(3.8) \quad a_1 = (-0.35, 0), \quad a_2 = (-k\Delta x, 0), \quad a_3 = (0.35, 0)$$

with  $\rho_c = 0.05$  for  $k \geq 0$ . Note that the critical distance  $\tilde{d}_c = 0.474650$  is less than distance between the two farthest center  $L = |a_1 - a_3| = 0.70$ . Here we have used the revised critical distance as presented in §3.3. In this case, the situations are divided into the following two situations.

- (a) A group of triplets, if  $|a_2 - a_3| \leq \tilde{d}_c$ ,
- (b) A co-rotating pair and independent unit spiral, if  $|a_2 - a_3| > \tilde{d}_c$ .

Burton et al. also pointed out in [1, §9.2] that the resultant growth rate is always that of the most active independent group. This suggests that the growth rate of case (b) should be  $R^{(2)}(|a_1 - a_2|)$ . However, if the estimate



by [1] were valid, the growth rate by this group with respect to  $|a_1 - a_2|$  would have a unnatural discontinuity at  $|a_1 - a_2| = L - \tilde{d}_c$  as in left figure of Figure 3.8. Hence, we examine the growth rate of triplets at (3.8) with  $\rho_c = 0.05$ , aiming at revealing whether or not such a discontinuity appears. Our results are presented in the right plot in Figure 3.8.

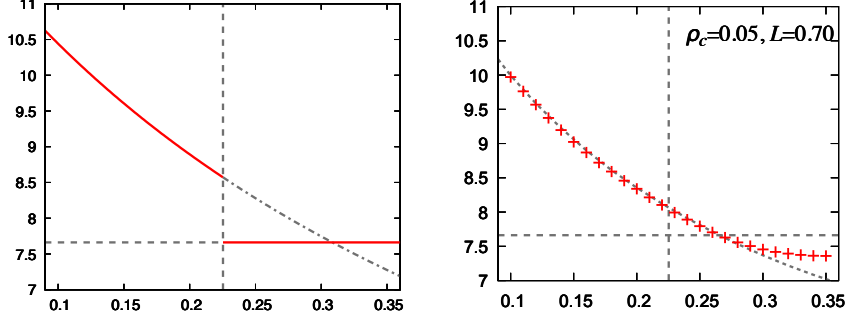


FIGURE 3.8. Comparison between estimates by [1] (left figure) and numerical simulations (right figure) with  $\rho_c = 0.05$ . The horizontal axis corresponds to  $|a_1 - a_2|$  and the vertical axis is the rate. The dashed vertical line shows the distance  $|a_1 - a_2| = 0.70 - \tilde{d}_c$  (i.e.,  $|a_2 - a_3| = \tilde{d}_c$ ) with  $\rho_c = 0.05$ . The dashed horizontal line shows the rate  $R^{(3)}(0.70) \approx 7.662046$  given by (3.7). The chain line and the dotted line denote  $R^{(2)}$  (left figure) and  $R_{\Delta}^{(2)}$  obtained in §3.3, respectively.

The right figure in Figure 3.8 presents numerical results of the growth rate by (3.8) with  $\rho_c = 0.05$  for  $0 \leq k \leq 25$  with respect to  $d := |a_1 - a_2| = 0.35 - k\Delta x$ . The growth rates are estimated in the time interval  $[0.3, 1.0]$ . We also plot  $R_{\Delta}^{(2)}(|a_1 - a_2|)$  as the dotted line. The growth rates of the triplets follows closely the values of  $R_{\Delta}^{(2)}(|a_1 - a_2|)$  on the region where  $R_{\Delta}^{(2)}(|a_1 - a_2|) > R^{(3)}(L)$  even if the centers are sufficiently close to be regarded as the group in the sense of [1] (to the right of the dashed vertical line). However, when  $R_{\Delta}^{(2)}$  becomes smaller than  $R^{(3)}(0.70)$  (indicated by the dashed horizontal line), the growth rate of the triplets becomes larger than  $R_{\Delta}^{(2)}$ . Results similar to the above are obtained with the following setups:

- (i)  $\rho_c = 0.06$ ,  $a_1 = (-0.35, 0)$ ,  $a_2 = (-k\Delta x, 0)$ ,  $a_3 = (0.35, 0)$  for  $-25 \leq k \leq 0$ ,
- (ii)  $\rho_c = 0.05$ ,  $a_1 = (-0.40, 0)$ ,  $a_2 = (-k\Delta x, 0)$ ,  $a_3 = (0.40, 0)$  for  $-30 \leq k \leq 0$ .

See Figure 3.9.

We take the normalized distance  $|R_{\Delta}(d) - R^{(2)}(d)|/R^{(2)}(d)$  between the numerical growth rates  $R_{\Delta}(d)$  of the triplets and  $R_{\Delta}^{(2)}(d)$ , which is presented

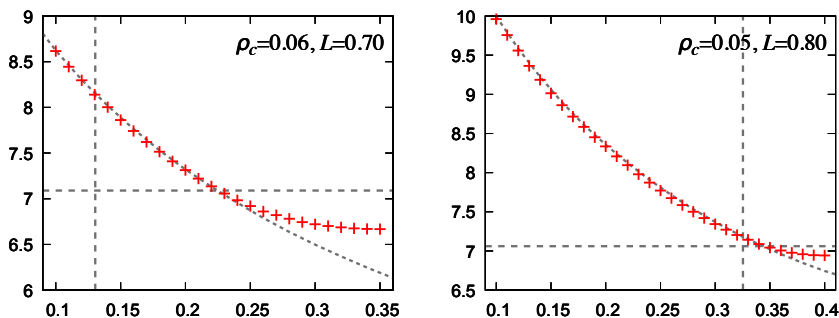


FIGURE 3.9. Growth rates of the triplets with case (i) and (ii). The horizontal and vertical dashed line respectively denotes  $R^{(3)}(L)$  and  $|a_1 - a_2| = L - \tilde{d}_c$  for each cases.

in Figure 3.10. Note that we choose  $s = 1$ , i.e.,  $\Delta x = 0.01$  for the consistency of numerical results, but we calculate  $R_{\Delta}^2(d)$  with the linear interpolation for  $d = 0.11, 0.13, \dots, 0.35$ . One can find that the growth rates are quite separated from  $R_{\Delta}^{(2)}$  if  $d$  is larger than where  $R_{\Delta}^{(2)}$  goes across  $R^{(3)}(L)$ .

In the simulations with case (i), note that the triplets should be regarded as a co-rotating group of triplet if  $k \leq 21$  ( $|a_2 - a_3| \leq 0.56$ ). However, the growth rate becomes quite larger than that by a co-rotating pair if  $k \leq 13$ , where  $R^2(d)$  is also smaller than  $R^3(0.7)$  with  $\rho_c = 0.06$  if  $d \geq 0.22$ . The case (ii) also proposes that the growth rates become faster than those by a co-rotating pair provided that  $k \leq 6$  although the triplets should be regarded as a co-rotating group of triplet if  $k \leq 2$  ( $|a_2 - a_3| \leq 0.38$ ). One can find in the both cases that the growth rate by a co-rotating triplet is faster than a co-rotating pair, however, slower than that calculated by (3.7).

From our numerical simulations, we have the following predictions (note that the quantities are simulations by (3.8) with  $\rho_c = 0.05$ ):

- The growth rate seems to decay smoothly for  $d \geq 0.23$  although the triplets are classified as a group if  $0.23 \leq d \leq 0.35$ .
- The growth rate by the triplets becomes smaller than  $R^{(3)}(0.70)$  if  $d \geq 0.27$ , however it continues to decay. Note that  $R_{\Delta}^{(2)}(d)$  is also smaller than  $R^{(3)}(0.70)$  if  $d \geq 0.27$ .
- The growth rate is essentially larger than  $R_{\Delta}^{(2)}(d)$  if  $d \geq 0.27$ .

In summary, distribution of the screw dislocations on a line influence to the growth rate of the whole group. In particular, if the group can be regarded as sub groups of more closely positioned centers, then the resultant growth rate should be that of the sub group with highest growth rate. The quantity  $R^{(N)}(L)$  possibly plays a role of threshold changing the mode of the evolution. However, we find no estimate for (3.8) if  $R_{\Delta}^{(2)}(d) < R^{(3)}(L)$ .

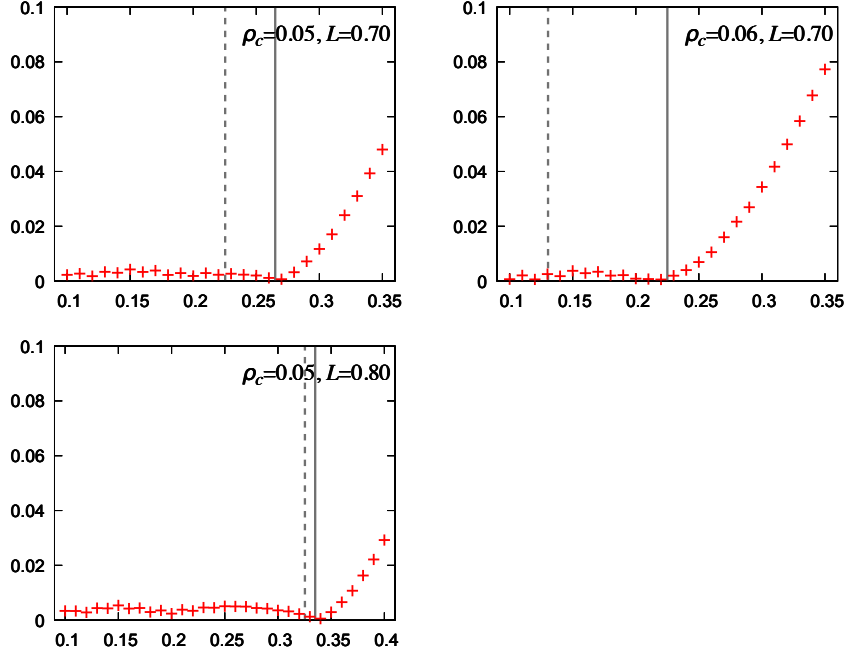


FIGURE 3.10. Normalized distances  $|R_\Delta(d) - R_\Delta^{(2)}(d)|/R_\Delta^{(2)}(d)$  with  $\rho_c = 0.05$ ,  $L = 0.7$ ,  $\rho_c = 0.06$ ,  $L = 0.7$ , and  $\rho_c = 0.05$ ,  $L = 0.8$ , respectively. The dashed lines are at  $L - \tilde{d}_c$ , and the solid lines at  $|a_1 - a_2| = 0.265$  (top),  $0.225$  (middle) or  $0.335$  (bottom) approximately denote the distance where  $R_\Delta^{(2)}$  goes across  $R_\Delta^{(3)}(L)$  in each cases.

As supplementary evidences to the above assertion, we present some examples of calculation of the growth rates for 4 co-rotating screw dislocations as in [9]. Recall the situation of the simulations: 4 co-rotating screw dislocations are located at

$$a_1 = (-a, 0), \quad a_2 = (-b, 0), \quad a_3 = (b, 0), \quad a_4 = (a, 0)$$

with

- (a)  $a = 0.06$  and  $b = 0.02$ ,
- (b)  $a = 0.15$  and  $b = 0.11$ .

The evolution equation is

$$V = 5(1 - 0.02\kappa),$$

i.e.,  $v_\infty = 5$  and  $\rho_c = 0.02$ . We choose the initial steps as

$$\begin{aligned} a_1 &: \{a_1 + (-r, 0); r > 0\}, \\ a_2 &: \{a_2 + (0, -r); r > 0\}, \\ a_3 &: \{a_3 + (0, r); r > 0\}, \\ a_4 &: \{a_4 + (r, 0); r > 0\}. \end{aligned}$$

See [9] for the details of the initial data, and the profiles of spiral steps at  $t = 0.5$ . Profiles are slightly different from each other. We now give a classification if these situations are a group of 4 co-rotating screw dislocations, or 2 pairs from a view point of the growth rates. See Figure 3.11 for the

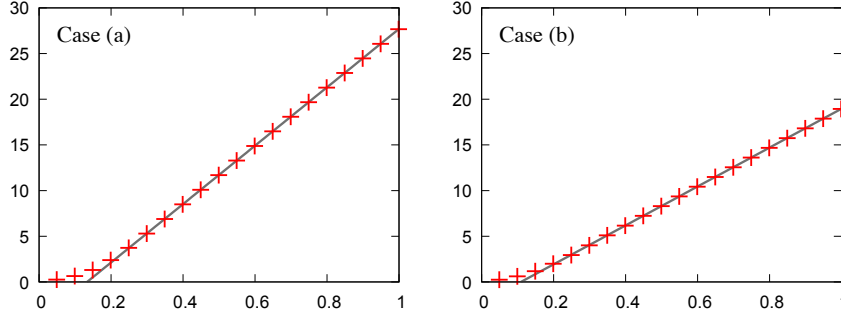


FIGURE 3.11. Graphs of  $H(t)$  by 4 screw dislocations (a)  $(\pm 0.06, 0)$  and  $(\pm 0.02, 0)$  (left), or (b)  $(\pm 0.15, 0)$  and  $(\pm 0, 11, 0)$  (right). The points denote the data of  $H(t)$  per the time span  $\Delta t = 0.05$ , and solid lines denote the fitting line by the data of  $H(t)$  in  $[0.3, 1]$ .

data plots of  $H(t)$  on these simulations. Each fitting line is as follows;

$$\begin{aligned} \text{(a)} \quad H(t) &\approx 31.96154528t - 4.26148724, \\ \text{(b)} \quad H(t) &\approx 21.29516137t - 2.33023461. \end{aligned}$$

Then, the growth rate of the case (a) is  $R_{\Delta,1} = 31.96154528$ , and that of the case (b) is  $R_{\Delta,2} = 21.29516137$ . The growth rate  $R^{(0)}$  with  $v_\infty = 5$ ,  $\rho_c = 0.02$  is

$$R^{(0)} = \frac{5\omega_1}{0.04\pi} \approx 13.168403.$$

The possibility of the classification (a) is

- (a1) a group of  $\{a_1, a_2, a_3, a_4\}$  with length  $L = 0.12$ ,
- (a2) a group of  $\{a_1, a_2, a_3\}$  and an independent  $\{a_4\}$ ,
- (a3) a pair of pairs  $\{a_1, a_2\}$  and  $\{a_3, a_4\}$ .

Then, each growth rate is calculated as follows.

$$\begin{aligned} \text{(a1)} \quad R^{(4)}(0.12) &= \frac{4}{1 + 0.12\omega_1/(0.02\pi)} R^{(0)} \approx 32.273849, \\ \text{(a2)} \quad R^{(3)}(0.08) &= \frac{3}{1 + 0.08\omega_1/(0.02\pi)} R^{(0)} \approx 27.793385, \\ \text{(a3)} \quad R &:= \frac{2}{1 + 0.08\omega_1/(0.02\pi)} R^{(2)}(0.04) \approx 30.608752. \end{aligned}$$

For case (a) one can find  $R^{(4)}(0.12)$  is the closest to  $R_{\Delta,1}$ . So case (a) should be regarded as a group of four co-rotating screw dislocations. Case (b), on the other hand, should be regarded as two independent (non-interacting) pairs  $\{a_1, a_2\}$  and  $\{a_3, a_4\}$  since  $a_2$  and  $a_3$  are disconnected in the sense that  $|a_2 - a_3| = 0.22 > \bar{d}_c$ . Thus, the growth rate should be estimated as  $R^{(2)}(0.04) \approx 21.753470$ . Even if we regard case (b) as a group of four screw dislocations on a line of length 0.30, (3.7) gives  $R^{(4)}(0.30) \approx 20.414480$ , which is farther than  $R^{(2)}(0.04)$ . Similarly, if we treat  $\{a_1, a_2\}$  and  $\{a_3, a_4\}$  as two effective pairs of centers, we obtain

$$R = \frac{2}{1 + 0.26\omega_1/(0.02\pi)} R^{(2)}(0.04) \approx 18.361125$$

by calculation similar to (a3). Note that the centers of the pair in this case should be regarded as  $(\pm 0.13, 0)$ .

**3.6. Complex group.** According to [1] the growth rate of crystal surface by several screw dislocations, could be estimated systematically by analyzing groups of screw dislocations independently. In essence, dislocations are collected into disjoint subsets. We shall refer to each of such subsets as a group. Inactive pairs are discarded from the groups. In each group, any dislocation center is no farther than  $d_c$  distance away from another dislocation center in the same group. Each group can be assigned a strength  $n$ , which is defined as

$$n = n_+ - n_-,$$

where  $n_+$  or  $n_-$  are number of single screw dislocations which has counter-clockwise or clockwise rotational orientations provided that the steps evolve, respectively. By the signed number  $m_j$  of screw dislocations defined as in §2.1 or [9], we represent  $n$  as

$$n = \sum_{j \in \Lambda} m_j,$$

where  $\Lambda$  is the set of numbers of screw dislocations in the group. It is mentioned in [1] that if  $n = 0$ , then the growth rate by the group is approximately the same as that of the unit spiral; otherwise,  $n \neq 0$ , the growth rate is  $|n|$  times that of the unit spiral.

Thus the effective growth rate of each group of dislocations can be estimated. The growth rate of the surface is then estimated by the maximum

of these effective growth rates. Of course, in our analysis, we use the revised critical distance  $\tilde{d}_c$  as defined in (3.6) for grouping the centers.

Motivated by the above speculation, we study numerically the growth rates of a surface consisting of two groups of dislocations which are getting closer in distance. In particular, we consider the case in which one the groups consist of a single dislocation. For example, we consider the evolution of the surface with

$$(3.9) \quad a_1 = (0, -0.05; 1), \quad a_2 = (0, 0.05; 1), \quad a_3 = (k\Delta x, 0; -1) \text{ for } k \geq 0$$

with the evolution equation

$$(3.10) \quad V = 6(1 - 0.04\kappa),$$

i.e.,  $v_\infty = 6$ ,  $\rho_c = 0.04$ . In (3.9), we have expressed the screw dislocation  $a_j$  as the triplet  $(p_j, q_j; m_j)$  where  $(p_j, q_j)$  is the coordinates of dislocation, and  $m_j \in \{\pm 1\}$  is the rotational orientation. By [1] the growth rate can be estimated by:

- (c1) If  $|a_1 - a_3| \geq \tilde{d}_c$ , the growth rate should be  $\max\{R^{(2)}(0.10), R^{(0)}\} = R^{(2)}(0.10)$  with  $\rho_c = 0.04$ .
- (c2) If  $2\rho_c \leq |a_1 - a_3| < \tilde{d}_c$ , then  $\{a_1, a_2, a_3\}$  are all in the same group and  $s = 1$  on this group. The growth rate should be  $1 \times R^{(0)} = R^{(0)}$ .
- (c3) If  $|a_1 - a_3| < 2\rho_c := 0.08$ , then  $a_1$  and  $a_3$  form an inactive pair, and only  $a_2$  influences the growth rate. The growth rate should be  $R^{(0)}$ .

Note that in this case  $|a_1 - a_3| = \sqrt{0.05^2 + (k\Delta x)^2}$ , so that the first case appears when

$$k\Delta x \geq a^{**} := \sqrt{\tilde{d}_c^2 - 0.05^2} \approx 0.376390,$$

and the third case appears when

$$k\Delta x = a^* := \sqrt{(2\rho_c)^2 - 0.05^2} \approx 0.062450.$$

Hence, we obtain the estimate of the growth rate by (3.9) as in the top-left figure of Figure 3.12. For this speculations, our interests in this section are as follows.

- (i) Why the effective distance is  $\tilde{d}_c$  even for pair of screw dislocations with opposite rotational orientations? The effective line between the pair with opposite rotational orientations should be shorter than  $2\rho_c$ .
- (ii) Dependency of the length of effective line to the growth rate. We think the discontinuity as shown in Figure 3.12 is unnatural.

The top-right figure in Figure 3.12 shows the graph of the numerical growth rate  $R_\Delta$  in this situation, which is calculated on a time interval  $[0.7, 2.0]$ . The horizontal axis means  $k\Delta x$ . The horizontal dashed lines in the right figure are drawn at  $R^{(0)} \approx 7.901042$  and  $R_\Delta^{(2)}(0.10) \approx 11.904457$ . The vertical dashed lines are drawn at  $k\Delta x = a^*$  and  $k\Delta x = a^{**}$ . The bottom figure is the enlarged one of numerical results around 11.9 of  $y$ -axis.

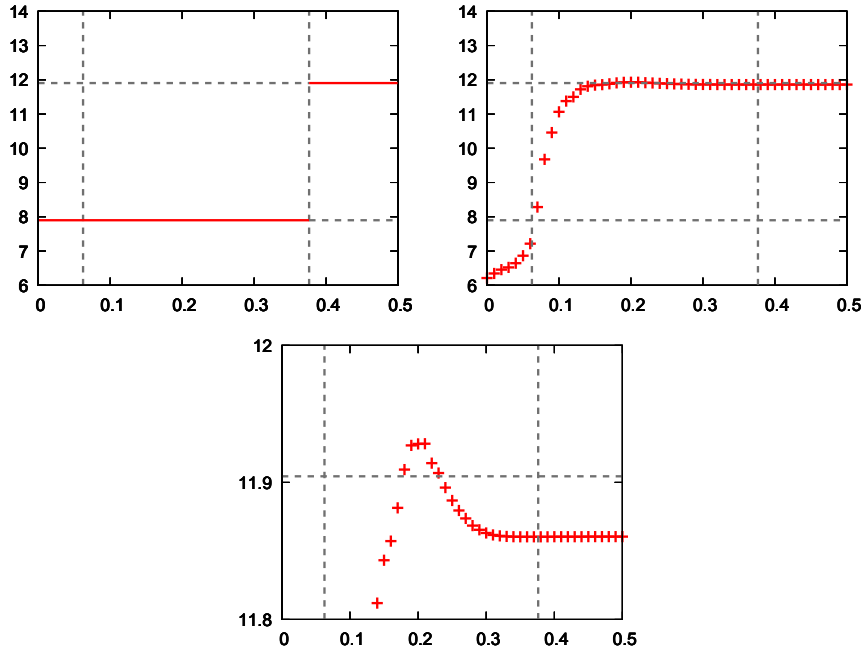


FIGURE 3.12. The estimate by [1] of the growth rate by (3.9) (top-left) and its numerical results (top-right). The horizontal axis means  $k\Delta x$ , and the vertical dashed line are located at  $k\Delta x = a^*$  or  $a^{**}$ . In the bottom figure, we zoom in the numerical results around 11.9 of  $y$ -axis.

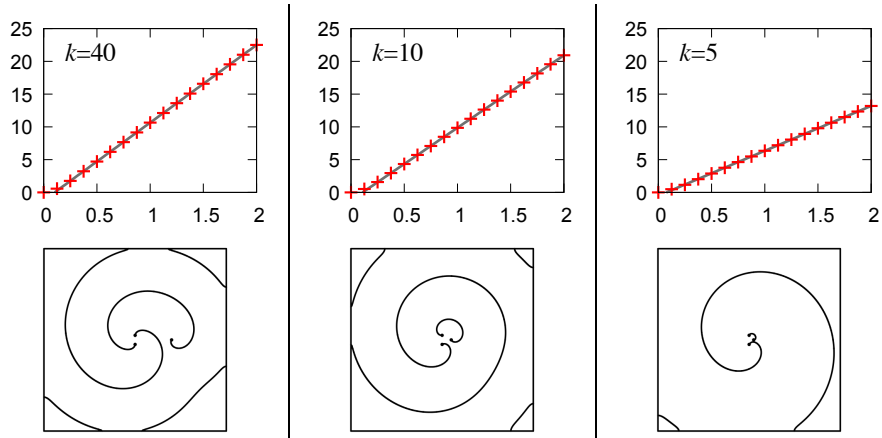


FIGURE 3.13. Graphs of  $H(t)$  and profiles of spirals at  $t = 2$  with  $s = 1$  ( $\Delta x = 0.01$ ) for each case of (c1), (c2), (c3) as  $k = 40, 10, 5$ , respectively.

In Figure 3.13 we present three numerical simulations, using  $k = 40, 10, 5$  corresponding to cases (c1)–(c3). The numerically observed growth rates are

$$R_{\Delta} = 6.863008, \quad R_{\Delta} = 11.064736, \quad R_{\Delta} = 11.860357.$$

On the other hand, we have

$$R^{(0)} \approx 7.901042, \quad R^{(2)}(0.10) \approx 12.507902, \quad R_{\Delta}^{(2)}(0.10) \approx 11.904457,$$

where  $R^{(2)}(0.10)$  is calculated with (3.4), and  $R_{\Delta}^{(2)}(0.10)$  is the numerical result obtained in §3.3. There seem to be quite some discrepancy between the presented computation and the one predicted by [1].

We now summarize the numerical results in Figure 3.12 as follows.

- The growth rate keeps its quantity around  $R_{\Delta}^{(2)}(|a_1 - a_2|)$  until  $k\Delta x \geq 0.15$ . Note that  $|a_1 - a_3| \approx 0.158114$  for  $k\Delta x = 0.15$  is close to  $4\rho_c = 0.16$ .
- The growth rate is smaller than  $R^{(0)}$  if  $|a_1 - a_3| < 2\rho_c$ .
- The growth rate attains its maximum at  $2\rho_c < |a_1 - a_3| < \tilde{d}_c$ , and monotone decrease for  $|a_1 - a_3|$  over the distance achieving the maximal growth rate.

The profile of the growth rate at  $|a_1 - a_3| > 2\rho_c$  looks like the subplots in Figure 3.6. So, similar overshooting of growth rates as a pair with opposite rotational orientation may appear if a group includes an accelerating pair with opposite rotations. On the other hand, the second fact of the above implies that an inactive pair in a group of screw dislocations may reduce the growth rate of the group.

In this section, the growth of surface by a triplet with co-rotating pair and other one having opposite rotational orientation is examined. In the numerical simulations, we fix a co-rotating pair of spirals, and study the growth rate as the center of the third spiral, with opposite rotational orientation, approaches the former two. We observed that if the distance,  $L$ , between center of the third spiral and those of the co-rotating ones is larger than the critical distance (for an inactive pair of spirals), then the growth rate tends rapidly to the rate of the co-rotating pair, as  $L$  becomes larger. If  $L$  is too small, then the growth rate is less than that of the unit spiral.

#### 4. CONCLUSION AND REMARKS

In this paper, we study analytically and numerically the growth rate of a crystal surface growing by several screw dislocations. We carefully compare our estimates and simulation results with some of the classical cases in the literature. We obtained new estimates on the growth rates for several different configurations (co-rotating pairs of spirals, spirals whose centers are co-linear, and groups of spirals), and we showed that these new rates were in agreement with the numerical simulations computed by the level set method proposed in [9]. We gave a new definition of the critical distance



(of co-rotating pair) with the view point of effective growth rate. We also gave an improved estimate of the growth rate by a co-rotating pair with a estimate of the rotating single spiral by Ohara-Reid [8]. By arguments used in the above two items, we concluded that the critical distance by [1] is too small. We found that the growth rate by a pair of opposite rotational screw dislocations, attains the maximum with the distance between the spiral centers is between  $3.5\rho_c$  and  $4\rho_c$ . We found that the distribution of screw dislocations on a line influences to the growth rate. We carefully studied how the growth rate depends on the distribution. For general group of spirals, we found that the growth rate can be studied systematically by the rates of the "effective" sub-groups of centers, partitioned by the inter-distances.

## REFERENCES

- [1] W. K. Burton, N. Cabrera, and F. C. Frank. The growth of crystals and the equilibrium structure of their surfaces. *Philosophical Transactions of the Royal Society of London. Series A. Mathematical and Physical Sciences*, 243:299–358, 1951.
- [2] N. Cabrera and M. M. Levine. Xlv. on the dislocation theory of evaporation of crystals. *Philosophical Magazine*, 1(5):450–458, 1956.
- [3] Yoshikazu Giga. *Surface evolution equations: A level set approach*, volume 99 of *Monographs in Mathematics*. Birkhäuser Verlag, Basel, 2006.
- [4] Shun'ichi Goto, Maki Nakagawa, and Takeshi Ohtsuka. Uniqueness and existence of generalized motion for spiral crystal growth. *Indiana University Mathematics Journal*, 57(5):2571–2599, 2008.
- [5] Alain Karma and Mathis Plapp. Spiral surface growth without desorption. *Phys. Rev. Lett.*, 81:4444–4447, Nov 1998.
- [6] Ryo Kobayashi. A brief introduction to phase field method. *AIP Conf. Proc.*, 1270:282–291, 2010.
- [7] Hitoshi Miura and Ryo Kobayashi. Phase-field modeling of step dynamics on growing crystal surface: Direct integration of growth units to step front. *Crystal Growth & Design*, 15(5):2165–2175, 2015.
- [8] M. Ohara and R. C. Reid. *Modeling Crystal growth rates from solution*. Prentice-Hall Inc., 1973.
- [9] T. Ohtsuka, Y.-H.R. Tsai, and Y. Giga. A level set approach reflecting sheet structure with single auxiliary function for evolving spirals on crystal surfaces. *Journal of Scientific Computing*, 62(3):831–874, 2015.
- [10] Takeshi Ohtsuka. A level set method for spiral crystal growth. *Advances in Mathematical Sciences and Applications*, 13(1):225–248, 2003.
- [11] Takeshi Ohtsuka. Evolution of crystal surface by a single screw dislocation with multiple spiral steps. *Sūrikaisekikenkyūsho Kōkyūroku*, (1924):11–20, 2014. Mathematical analysis of pattern formation arising in nonlinear phenomena (Kyoto, 2013).
- [12] Takeshi Ohtsuka. Inactive pair in evolution of an opposite rotating pair of spirals by eikonal-curvature flow equations. in preparation.
- [13] Stanley Osher and Ronald P. Fedkiw. Level set methods: an overview and some recent results. *J. Comput. Phys.*, 169(2):463–502, 2001.
- [14] Stanley Osher and James A. Sethian. Fronts propagating with curvature-dependent speed: algorithms based on Hamilton-Jacobi formulations. *J. Comput. Phys.*, 79(1):12–49, 1988.
- [15] J. A. Sethian. *Level set methods and fast marching methods*. Cambridge University Press, Cambridge, second edition, 1999. Evolving interfaces in computational geometry, fluid mechanics, computer vision, and materials science.

4-2, ARAMAKI-MACHI, MAEBASHI, GUNMA 371-8510, JAPAN

THE UNIVERSITY OF TEXAS AT AUSTIN, USA AND KTH ROYAL INSTITUTE OF TECHNOLOGY, SWEDEN

KOMABA 3-8-1, MEGURO-KU, TOKYO 153-8914, JAPAN